

PACS numbers: 71.15.Mb, 71.15.Nc, 78.20.Ci, 78.30.-j, 78.40.-q, 78.67.Sc, 82.35.Np

Design of PEO/NiO/In₂O₃ Structures and Tailoring the Optical and Electronic Characteristics for Electronic Devices

Huda Bukheet Hassan¹, Hayder M. Abduljalil², and Ahmed Hashim¹

¹College of Education for Pure Sciences,
Department of Physics,
University of Babylon,
Hillah, Iraq

²College of Science,
Department of Physics,
University of Babylon,
Hillah, Iraq

In present work, the new PEO/NiO/In₂O₃ structures are designed to be employed in various optical and electronic approaches. The structural, optical, and electronic characteristics of new PEO/NiO/In₂O₃ structures are studied. The effect of increasing the number of atoms on the geometrical, electrical, and spectral features of PEO/NiO/In₂O₃ structures is investigated using the Gaussian 0.9 software and Gaussian View 0.5, as well as density functional theory (SDD basis set) for the geometrical, electronic, and spectroscopic properties of PEO/NiO/In₂O₃ (with 85 atoms). Improved geometrical optimization is done for the geometrical features (bonds and angles). In addition to spectrum qualities, electronic properties include ionization potential, electron affinity, chemical hardness, chemical softness, electronegativity, total energy, energy gap, electrophilicity as well as the IR and UV-visible spectra. When the number of atoms in the investigated structure is increased, it has a direct effect on all of its attributes. Finally, acquired results for the new PEO/NiO/In₂O₃ structures show that they can be used in a variety of modern applications.

У цій роботі нові структури поліоксидетилен/NiO/In₂O₃ (ПОЕ/NiO/In₂O₃) створено для використання в різних оптичних та електронних підходах. Досліджено структурні, оптичні та електронні характеристики нових структур ПОЕ/NiO/In₂O₃. Досліджено вплив збільшення кількості атомів на геометричні, електричні та спектральні особливості структур ПОЕ/NiO/In₂O₃ за допомогою програмного забезпечення Gaussian 0.9 і Gaussian View 0.5, а також теорії функціоналу густини (з базисним набором SDD) для геометричних, електронних і спектроскопічних властивостей ПОЕ/NiO/In₂O₃ (з 85 атомами). Поліпшену геометричну оптимі-

зацію виконано для геометричних особливостей — зв'язків і кутів. Крім спектральних якостей, електронні властивості включають потенціал йонізації, спорідненість електронів, хемічну твердість, хемічну м'якість, електронегативність, повну енергію, енергетичну щільність, електрофільність, а також спектри в інфрачервоному діапазоні та у видимому й ультрафіолетовому діапазонах світла. Коли кількість атомів у досліджуваній структурі збільшується, це безпосередньо впливає на всі її ознаки. Одержані результати для структур ПОЕ/NiO/In₂O₃ показують, що вони можуть бути використані в різних сучасних застосуваннях.

Key words: poly(ethylene oxide), metal oxide, nanocomposites, optical properties, electronic devices.

Ключові слова: поліоксиетилен, оксид металів, нанокомпозити, оптичні властивості, електронні прилади.

(Received 5 October, 2022)

1. INTRODUCTION

Polymer nanocomposites (PNCs) may be defined as a mixture of two or more materials, where the matrix is a polymer and the dispersed phase has at least one dimension smaller than 100 nm. In the last decades, it has been observed that the addition of low contents of these nanofillers into the polymer can lead to improvements in their mechanical, thermal, barrier and flammability properties, without affecting their processability. The ideal design of a nanocomposite involves individual nanoparticles homogeneously dispersed in a matrix polymer. The dispersion state of nanoparticles is the key challenge in order to obtain the full potential of properties enhancement. This uniform dispersion of nanofillers can lead to a large interfacial area between the constituents of the nanocomposites. The reinforcing effect of filler is attributed to several factors, such as properties of the polymer matrix, nature and type of nanofiller, concentration of polymer and filler, particle aspect ratio, particle size, particle orientation and particle distribution. Various types of nanoparticles, such as clays, carbon nanotubes, graphene, nanocellulose and halloysite, have been used to obtain nanocomposites with different polymers [1].

Poly(ethylene oxide) is a hydrophilic, biodegradable and semi-crystalline polymer with good biocompatibility and toughness [2]. PEO can be distinguished through its high thermal and chemical stability, high viscosity, and non-ionic, heat formative, good water solubility properties. PEO can also be identified through its flocculent thickening sustained-release lubrication that disperses fibres and retains water [3]. The properties of conducting polymer nano-

composites depend mainly on the nature of the association between inorganic and organic components.

Nickel oxide (NiO) is a *p*-type semiconductor with a variety of applications in optical, electronic and magnetic devices and this is because of the presence of Ni⁺ and Ni⁺⁺ in the metal oxide [4]. The introduction of NiO nanoparticles into the conjugated polymer greatly enhances the charge storage capacity in comparison to the parent polymer. This is mainly due to the morphology of the hybrid system in which the specific surface area, particle size and size distributions are significantly modified by the incorporation of metal nanoparticle [5].

Indium oxide (In₂O₃) is a technically very important transparent conductive oxide (TCO) substance. In₂O₃ is an *n*-type semiconductor with energy gap in the range from 3.6 to 3.72 eV. The In₂O₃ structure with crystalline form is b.c.c. (body-centred cubic) with a lattice constant of 10.11 Å [6].

This work aims to design of new PEO/NiO/In₂O₃ structures to employ in various optical and electronic approaches.

2. THEORETICAL PART

The HOMO (the highest energy occupied by electrons) and LUMO (the lowest energy occupied by electrons) are the main properties in arithmetic such as molecular interaction and molecular ability to adsorb photon light. According to Koopmans' theory, the band gap is given by [7]:

$$E_{\text{gap}} = E_{\text{LUMO}} - E_{\text{HOMO}}. \quad (1)$$

The ionization potential (*IP*) is difference between the positive energy $E(+)$ and the neutral one $E(n)$:

$$IP = E(+)-E(n). \quad (2)$$

The electron affinity (*EA*) is given as a function of both the neutral energy $E(n)$ and the negative energy $E(-)$:

$$EA = E(n) - E(-). \quad (3)$$

The energies of the frontier orbitals are determined as

$$IP = -E_{\text{HOMO}}, \quad (4)$$

$$EA = -E_{\text{LUMO}}. \quad (5)$$

Chemical hardness (η) measures the extent of resistance to the

transfer of charges. It is given as a function of electrons' numbers N and external potential $V(r)$ [8]:

$$\eta = \frac{1}{2} \left[\frac{\partial^2 E}{\partial N^2} \right]_V = S \left[\frac{\partial \mu}{\partial N} \right] = \frac{1}{2} \left[\frac{\partial X}{\partial N} \right]_V, \quad (6)$$

$$\eta = (IP - EA)/2. \quad (7)$$

Chemical softness (S) is a characteristic of molecules, which measures the chemical reactivity degree. It is a converse of chemical hardness (η) [9]:

$$S = \frac{1}{2\eta} = \left[\frac{\partial^2 N}{\partial E^2} \right]_V = \left[\frac{\partial N}{\partial \mu} \right]_V. \quad (8)$$

The chemical potential (K) μ , defined as [10]:

$$K = \left[\partial E / \partial N \right]_V, \quad (9)$$

where V is nuclei potential.

Then, we can determine the electronegativity using the relationship [8]

$$X = -K = -\left[\partial E / \partial N \right]_V. \quad (10)$$

It can be obtained by the average ionization energy and electron affinity [11]:

$$X = (IP + EA)/2. \quad (11)$$

According to Koopmans' theorem, 'it is defined as the negative value for average of the energy levels of the HOMO and LUMO' [12]:

$$X = -(E_{\text{HOMO}} + E_{\text{LUMO}})/2. \quad (12)$$

It measures the energy stability, when the structure gets additional electron charges from the environment, defined as electrophilic [13]:

$$\omega = \kappa^2 / 2\eta. \quad (13)$$

The electric dipole polarizability is the measure of the linear response of the electron density in the presence of an infinitesimal electric field F , and it represents a second-order variation in energy [14]. The polarizability is calculated by the following equation [15]:

$$\langle \alpha \rangle = (\alpha_{xx} + \alpha_{yy} + \alpha_{zz})/3. \quad (14)$$

3. RESULTS AND DISCUSSION

Density functional theory was used to simulate the relaxation of structure for the new PEO/NiO/In₂O₃ structures. Relaxation structure provided the bond length and angle between atoms.

Figure 1 represents geometrical model for the PEO/NiO/In₂O₃ structures.

Table 1 presents the geometric characteristics of PEO/NiO/In₂O₃ structures (85 atoms) including the lengths of bonds in [Å] and the

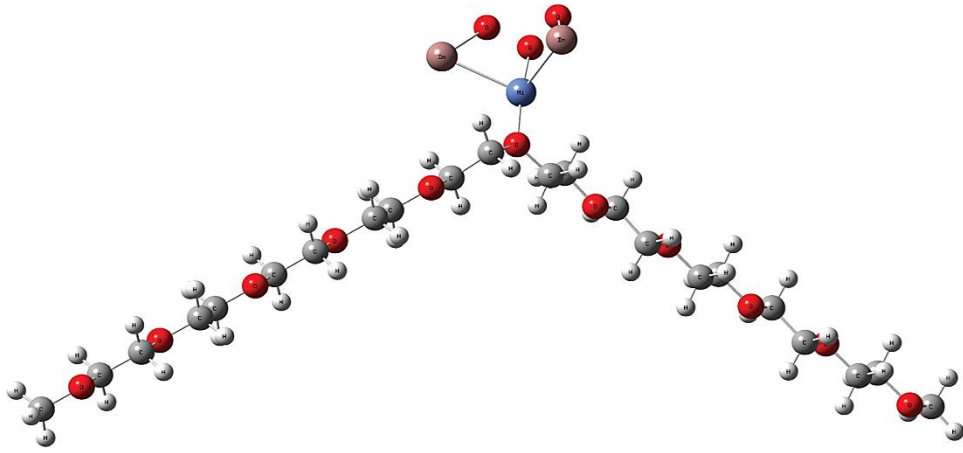


Fig. 1. Optimization of PEO/NiO/In₂O₃ (85 atoms) structures.

TABLE 1. Optimized bonds' lengths and optimized bonds' angles for nano-composites.

Values	Optimization parameters	Linear
Bonds, Å	(C-C)	1.52475
	(C-O)	1.45679
	(Ni-O)	1.90727
	(Ni-In)	2.72686
	(In-O)	2.11013
	(C-H)	1.10320
Angles, deg.	(H-C-H)	108.83735
	(C-O-C)	113.61651
	(O-Ni-In)	109.85133

angles of bonds in degrees using the DFT with B3LYP/6-31G level and the ‘Gaussian 09’ programs. The calculated bond values in this study are in good agreement with earlier theoretically estimated values [16–18].

The FTIR data are shown in Fig. 2 and Table 2. The interactions are depicted by the FTIR spectra of structures. Differences in spectra of PEO are caused by In_2O_3 , which include differences in a shift in many bonds and intensities.

The UV–Vis spectra are shown in Fig. 3 and Fig. 4. The electrical structure of the molecule determines the visible and ultraviolet spectra. The absorption intensity of new PEO/NiO/ In_2O_3 structures (85 atoms) has a greater UV–Vis spectrum, as shown in Figs. 3 and 4. As a result, absorption increases as the number of atoms grows. This is due to electrons’ shifting from the valence level to the conduction band at these energies, resulting in an increase in absorption due to the increased number of charge carriers [6, 22–26].

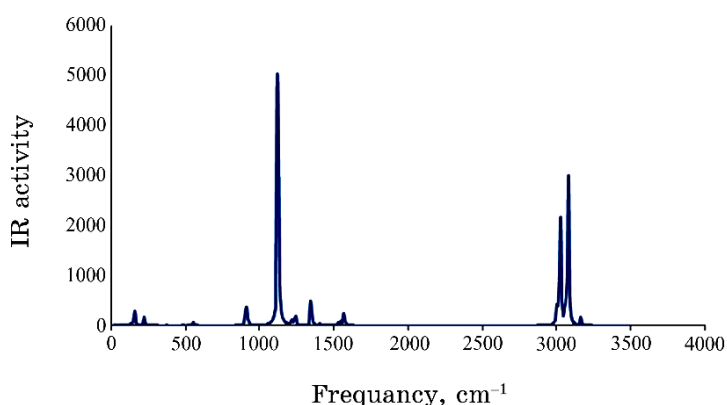


Fig. 2. IR spectra of new PEO/NiO/ In_2O_3 structures (85 atoms) by using B3LYP/SDD basis set.

TABLE 2. IR frequencies of new PEO/NiO/ In_2O_3 structures.

Assignment	Vibrational-mode type	Frequency, cm^{-1}	Typical vibrational frequency, cm^{-1}
C–O	Stretching	1002.08	1000–128 [19]
CH_2	In-plane bending	1352.80	1340–146 [19]
C–C	Stretching and bending	1058.13	700–1600 [18]
C–H	Symmetric stretching	3064.83	3020–308 [19]
C–O–C	Bending	1244.28	1238–129 [19]
Ni–O	Stretching	469.88	457–600 [20]
In–O	Stretching	469.18	441–583 [21]

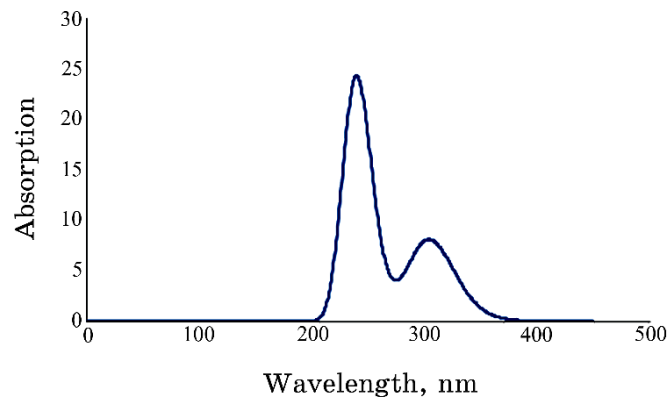


Fig. 3. UV-Vis spectrum for the PEO (85 atoms) by using B3LYP/6-31G.

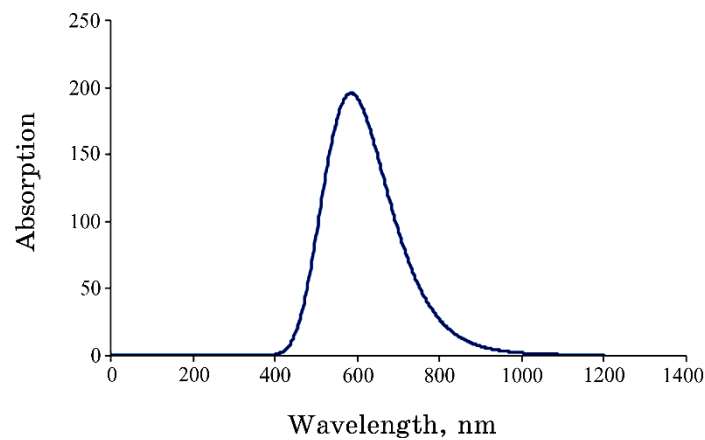


Fig. 4. UV-Vis spectrum for the new PEO/NiO/In₂O₃ structures (85 atoms) by using B3LYP/SDD.

TABLE 3. The values of HOMO, LUMO and energy gap in [eV] of new PEO/NiO/In₂O₃ structures.

Ribbon	HOMO, eV	LUMO, eV	Energy gap, eV
PEO	-6.7995	1.2679	8.0674
PEO-NiO	-3.9323	-1.3847	2.5476
PEO-NiO-In ₂ O ₃	-5.0972	-2.0641	3.0330

The energy gap for the new PEO/NiO/In₂O₃ structures (85 atoms) is shown in Table 3. The calculated energy gap diminishes as the number of atoms increases, according to the data.

The energy gap reduces with adding the NiO and NiO-In₂O₃. This

TABLE 4. Electronic-properties' values of new PEO/NiO/In₂O₃ structures.

Property	PEO	New PEO/NiO/In ₂ O ₃ structures
Total energy (<i>ET</i>)	-1692.8063 a.u.	-2093.4601 a.u.
Ionization potential (<i>IE</i>)	6.7995 eV	5.0972493 eV
Electron affinity (<i>EA</i>)	-1.2679 eV	2.0641 eV
Electronegativity (<i>EN</i>)	2.7658 eV	3.5806 eV
Chemical hardness (η)	4.0337eV	1.5165 eV
Chemical softness (<i>S</i>)	0.1239 eV	0.3297 eV
Chemical potential (<i>K</i>)	-2.7658 eV	-3.5806 eV
Electrophilicity (ω)	0.94821 eV	4.2269 eV
Dipole moment (Debye)	1.6673 eV	8.3365 eV

TABLE 5. The calculated α_{ave} and its components for the new PEO/NiO/In₂O₃ structures.

Polarizability, a.u.			
α_{xx} , a.u.	α_{yy} , a.u.	α_{zz} , a.u.	α_{ave} , a.u.
508.564	403.368	386.810	432.914

reduced energy gap indicates the presence of charge transfer complexes due to the defect formations in the polymer matrix. These defects create the localized levels in the energy gap [27–32].

Table 4 presents the results of the *ET* in [a.u.] and some electronic properties of PEO and new PEO/NiO/In₂O₃ structures calculated at the same level of theory. These properties are also including *IE*, *EA*, *EN*, η , ω and dipole moment.

Table 5 shows the polarizability average α_{ave} and its components in [a.u.] of new PEO/NiO/In₂O₃ structures.

Figure 5 show the three-dimensional distribution of HOMOs and LUMOs in the nanocomposites examined.

4. CONCLUSIONS

The validity of the B3LYP level with SDD density functional theory in investigating geometry optimization and calculating geometrical parameters (bonds' lengths and angles) was demonstrated.

FTIR studies show that there are no interactions between PEO–NiO and In₂O₃ nanoparticles' concentrations.

The optical absorbance of PEO–NiO nanocomposites increases with the increase in In₂O₃ nanoparticles' concentration.

In addition, one of the most notable outcomes of this research was the reduction of the energy gap. Because the HOMO and LUMO

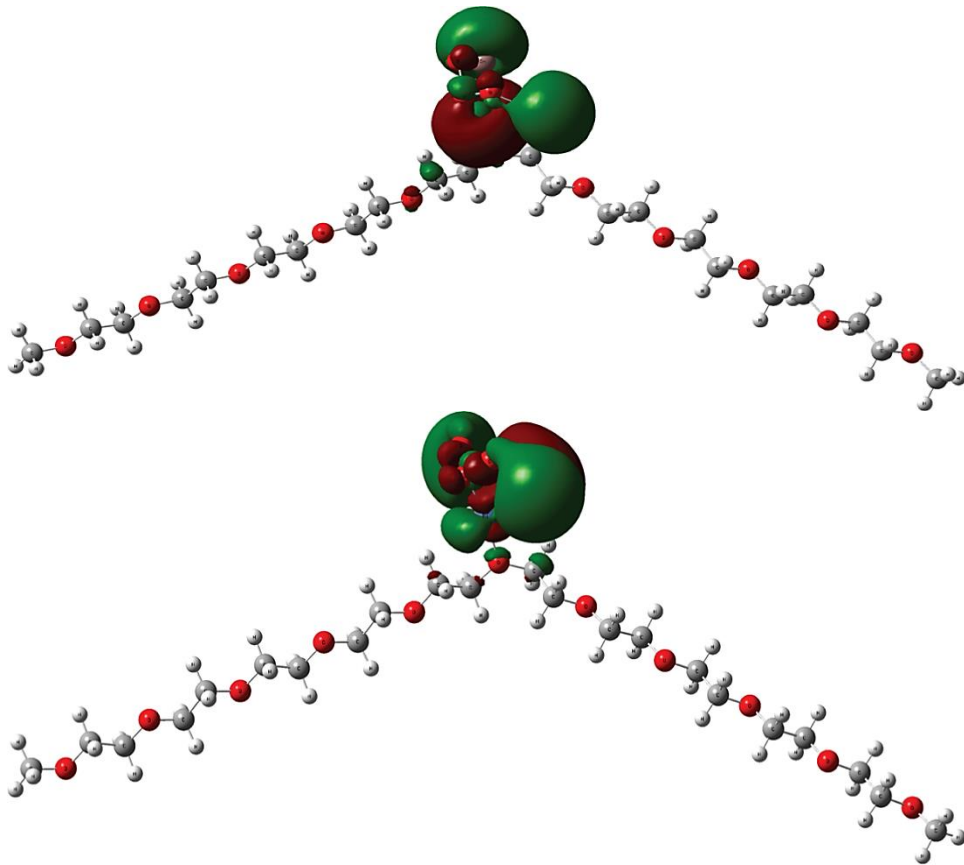


Fig. 5. The shape of HOMO (up) and LUMO (down) for the new PEO/NiO/In₂O₃ structures containing 85 atoms.

levels become progressively nearby, these nanocomposites are the closest to semiconductors.

Because the ionization potential decreases with the addition of nanoparticles to pure PEO, but the electronic affinity increases with the addition of nanoparticles to pure PEO, all of the examined nanocomposites require little energy to become cations.

The total ground state energy of the PEO has largest value of total energy in comparison with other nanocomposites, where ET is decreased with addition nanoparticles to pure PEO.

The hardness decreases with addition nanoparticles to the pure PEO; therefore, all the nanocomposites are softer, and this reduces the resistance of species to lose electrons.

The obtained results indicated that the new PEO/NiO/In₂O₃ structures could be used for various modern applications.

REFERENCES

1. A. D. de Oliveira and C. A. G. Beatrice, *Nanocomposites-Recent Evolutions* (IntechOpen: 2018), Ch. 6, p. 106;
<http://dx.doi.org/10.5772/intechopen.8132>
2. Y. Zare, H. Garmabi, and K. Y. Rhee, *Composites Pt. B: Engineering*, **144**: 1 (2018); <https://doi.org/10.1016/j.compositesb.2018.02.024>
3. M. O. Farea, A. M. Abdelghany, and A. H. Oraby, *RSC Advances*, **10**, No. 62: 37621 (2020).
4. M. T. Ramesan and V. Santhi, *Composite Interfaces*, **25**, No. 8: 725 (2018).
5. Y. Xie and X. Sha, *Synthetic Metals*, **237**: 29 (2018);
<https://doi.org/10.1016/j.synthmet.2018.01.011>
6. A. Hashim, *Journal of Inorganic and Organometallic Polymers and Materials*, **30**, No. 10: 3894 (2020); <https://doi.org/10.1007/s10904-020-01528-3>
7. M. Oftadeh, S. Naseh, and M. Hamadianian, *Computational and Theoretical Chemistry*, **966**, Nos. 1–3: 20 (2011).
8. W. J. Hehre, L. Radom, P. Schleyer, and J. A. Pople, *Ab initio Molecular Orbital Theory* (New York: Wiley-Interscience 1986).
9. P. W. Atkins and R. S. Friedman, *Molecular Quantum Mechanics* (Oxford University Press: 2010).
10. F. L. Riley, *Journal of the American Ceramic Society*, **83**, No. 2: 245 (2000).
11. D. Young, *A Practical Guide for Applying Techniques to Real World Problems* (Wiley: 2001).
12. J. Kohanoff and N. I. Gidopoulos, *Handbook of Molecular Physics and Quantum Chemistry* (2003), vol. 2 (pt. 5), p. 532.
13. K. Sadasivam and R. Kumaresan, *Computational and Theoretical Chemistry*, **963**, No. 1: 227 (2011).
14. A. J. Camargo, K. M. Honyrio, R. Mercadante, F. A. Molfetta, C. N. Alves, and A. B. da Silva, *Journal of the Brazilian Chemical Society*, **14**, No. 5: 809 (2003).
15. P. Udhayakala and T. V. Rajendiran, *Journal of Chemical, Biological and Physical Sciences*, **2**, No. 1: 172 (2011).
16. J. Chen, X. Wu, and A. Selloni, *Phys. Rev. B*, **83**, No. 24: 245204 (2011).
17. F. Creazzo, D. R. Galimberti, S. Pezzotti, and M. P. Gaigeot, *J. Chem. Phys.*, **150**, No. 4: 041721 86(2019).
18. M. Yu, C. S. Jayanthi, and S. Y. Wu, *arXiv preprint arXiv:0901.3567*: 1 (2009).
19. P. Atkins and J. De Paula, *Physical Chemistry for the Life Sciences* (USA: Oxford University Press: 2011).
20. J. M. Ramosa, M. C. Mauricio, C. C. Anilton Jr., V. Otavio, and A. T. S. Claudio, *Science Asia*, **37**: 247 (2011).
21. R. T. Rasheed, S. D. Al-Algawi, and S. Z. Tariq, *Iraqi Journal of Applied Physics*, **10**, No. 4: 15 (2014).
22. A. Hashim and Z. S. Hamad, *Egypt. J. Chem.*, **63**, No. 2: 461 (2020);
[doi:10.21608/EJCHEM.2019.7264.1593](https://doi.org/10.21608/EJCHEM.2019.7264.1593)
23. A. Hashim, *Journal of Inorganic and Organometallic Polymers and Materials*, **31**: 2483 (2021); <https://doi.org/10.1007/s10904-020-01846-6>
24. H. Ahmed, A. Hashim, and H. M. Abduljalil, *Ukr. J. Phys.*, **65**, No. 6: 533 (2020); <https://doi.org/10.15407/ujpe65.6.533>

25. F. L. Rashid, A. Hashim, M. A. Habeeb, S. R. Salman, and H. Ahmed, *Journal of Engineering and Applied Sciences*, **8**, No. 5: 137 (2013).
26. A. Hashim, *Opt. Quant. Electron.*, **53**: 1 (2021); <https://doi.org/10.1007/s11082-021-03100-w>
27. H. Ahmed and A. Hashim, *Transactions on Electrical and Electronic Materials*, **22**: 335 (2021); <https://doi.org/10.1007/s42341-020-00244-6>
28. A. Hazim, H. M. Abduljalil, and A. Hashim, *Transactions on Electrical and Electronic Materials*, **21**: 550 (2020); <https://doi.org/10.1007/s42341-020-00210-2>
29. A. Hazim, A. Hashim, and H. M. Abduljalil, *Trans. Electr. Electron. Mater.*, **21**: 48 (2019); <https://doi.org/10.1007/s42341-019-00148-0>
30. A. Hazim, H. M. Abduljalil, and A. Hashim, *Trans. Electr. Electron. Mater.*, **22**: 851(2021); <https://doi.org/10.1007/s42341-021-00308-1>
31. A. Hazim, H. M. Abduljalil, and A. Hashim, *Transactions on Electrical and Electronic Materials*, **22**: 185 (2021); <https://doi.org/10.1007/s42341-020-00224-w>
32. L. H. Gaabour, *Optics and Photonics Journal*, **10**: 197 (2020); [doi:10.4236/opj.2020.108021](https://doi.org/10.4236/opj.2020.108021)